Direct Numerical Simulation of Flame-Wall Interaction for a Forced Laminar Flame

R. Palulli, B. Jiang, J.E. Rivera, M. Talei, R.L. Gordon

Department of Mechanical Engineering, University of Melbourne, Victoria 3010, Australia

Abstract

This study investigates the flame-wall interaction of a two-dimensional (2D) laminar premixed flame using direct numerical simulation (DNS). The flame is excited by velocity perturbations at the inlet for a range of forcing frequencies. A single-step chemistry model is used to perform the simulations. The wall is assumed to be at the same temperature as the fresh gas.

The flame behavior is closely analyzed by using the contours of various parameters. This qualitative inspection is followed by determination of the Peclet number (Pe) in each case, in order to understand the nature of the flame quantitatively. A combination of the qualitative and quantitative methods provide more clarity on the various mechanisms involved in the flame-wall interaction.

The flame behavior is found to be different at low, intermediate and high frequencies. In particular, the flame behavior at intermediate frequencies is interesting as it showed a combination of head-on quenching and side-wall quenching during the flame interaction with the wall. Also, it can be inferred from the results that some conventional wall heat flux analysis methods may have to be modified to understand the flame behavior completely. The present study is a step towards performing a more realistic simulation to eventually account for the effects of turbulence and chemistry on the behavior of forced flames interacting with walls.

Introduction

Flame-wall interaction and quenching of flames near walls are present in both gas turbines and reciprocating engines. These are important phenomena due to their influence on the produced emission and fuel consumption. As a result, there is a great interest in the research community to better understand the flame behavior near walls.

Accurate experimental studies on flame-wall interaction introduce a tremendous challenge because quenching occurs very close to the wall and therefore it is difficult to measure the parameters of interest accurately [1, 6, 7]. Direct numerical simulation (DNS) is an alternative approach that can be used to study the fundamentals of flame-wall interaction in unprecedented detail e.g. [3, 5, 8, 9]. DNS has been widely used to study the influence of various key factors such as turbulence and/or chemistry in the context of flame-wall interaction e.g. [8, 9].

Early DNS studies on flame-wall interaction were performed for premixed flames in a head-on quenching configuration e.g. [9]. In this type of configuration, a propagating flame towards the wall is quenched when it is within a certain distance, known as quenching distance, from the wall. It was generally shown that a simple chemistry model is adequate for prediction of the flame behavior during its interaction the wall, when the wall temperature is below a certain threshold e.g. [11]. However, at higher wall temperatures, radical recombination plays an important role suggesting the need for using a detailed chemistry model.

Two-dimensional (2D) and three-dimensional (3D) DNSs have been also performed to study flame-wall interaction [3, 9]. For instance, Poinsot et al. [9] performed 2D DNS of flame-wall interaction of turbulent premixed flames. It was shown that the maximum heat flux and quenching distance results for turbulent cases were of the same order of magnitude in laminar cases. In a later study by Gruber et al. [8], the importance of flame thickening during flame-wall interaction was highlighted. It was also found that coherent turbulent structures have an important contribution on the wall heat transfer by pushing the hot products towards the wall. By performing a spectral analysis, they related the wall heat flux to the dominant time and length scales of these coherent turbulent structures.

Due to the high computational cost of DNS, 3D simulations of flame-wall interaction are limited to few cases, e.g. [3, 8]. However, laminar flames subjected to velocity perturbation under a range of forcing frequencies can be used as an alternative to study the transient effects during flame-wall interaction. Therefore, the present study aims to investigate this phenomenon for an acoustically forced flame using a single-step chemistry model.

Numerical Method

A 2D domain as shown in Figure 1 was used with 800 equally spaced grid points in the streamwise direction and 120 grids in the transverse direction. The number of grid points was chosen such that there are at least 10 grid points within the flame thickness. The upper boundary is the wall and is at the same temperature as the inlet. Inlet to the domain is at $X^+=x/L_{ref}=0$ from $Y^+=0.2$ to 1.2, where L_{ref} is the width of the inlet. A symmetry condition is applied to the bottom boundary. The flame is anchored at $X^+=0$ from $Y^+=0$ to 0.2, using tanh functions for both mass fraction and temperature. A parabolic velocity profile, corresponding to ducted laminar flows is induced at the inlet from $Y^+=0.2$ to 1.2. Sinusoidal velocity perturbations at 25% of the mean inflow velocity are provided at the inlet corresponding to St=0.01, 0.015, 0.02, 0.025, 0.03, 0.04, 0.05, 0.1, where $St = fL_{ref}/c_{ref}$ is the non-dimensional number corresponding to the frequency of excitation, f. The variable c_{ref} is the speed of sound in the fresh gas. Non-reflecting outflow at the left boundary was imposed using Navier-Stokes Characteristic Boundary Condition (NSCBC) [10]. The flame position was defined by the points where the reaction rate is maximum.
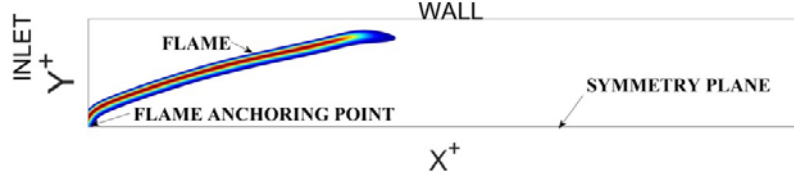
Figure 1:The computational Domain.

The DNS code NTMIX [4] was used to conduct the simulations. NTMIX is a high-order accurate solver that has been used to perform DNS of reactive flows using a single step chemistry e.g. [2, 12, 13]. It features a sixth-order compact scheme for spatial derivatives, combined with a third-order Runge–Kutta time integrator. The governing differential equations are as shown below [4]:

$$\frac{\partial \rho}{\partial t} + \frac{\partial}{\partial x_i}(\rho u_i) = 0, \tag{1}$$

$$\frac{\partial \rho e_t}{\partial t} + \frac{\partial}{\partial x_i}[(\rho e_t + p)u_i] = \frac{\partial}{\partial x_j}(u_i . \tau_{ij}) - \frac{\partial q_i}{\partial x_i} + Q\dot{\omega}, \tag{2}$$

$$\frac{\partial \rho u_i}{\partial t} + \frac{\partial}{\partial x_j}(\rho u_i u_j) + \frac{\partial p}{\partial x_i} = \frac{\partial \tau_{ij}}{\partial x_j}, \tag{3}$$

$$\frac{\partial (\rho \widetilde{Y_k})}{\partial t} + \frac{\partial}{\partial x_i}(\rho \widetilde{Y_k} u_i) = \frac{\partial}{\partial x_j}\left(\rho D_k \frac{\partial \widetilde{Y_k}}{\partial x_j}\right) - \dot{\omega}_k, \tag{4}$$

where $e_t = \frac{1}{2} . \sum_{k=1}^{3} u_k^2 + \frac{p}{\rho(\gamma-1)}, p = \rho RT,$

$$\tau_{ij} = \mu . \left(\frac{\partial u_i}{\partial x_j} + \frac{\partial u_j}{\partial x_i} - \frac{2}{3}\delta_{ij}\frac{\partial u_k}{\partial x_k}\right),$$

$$Q = \left(\frac{\alpha}{1-\alpha}\right)C_p T_1, \ \dot{\omega} = \Lambda \rho \widetilde{Y} exp\left(\frac{-\beta(1-\theta)}{1-\alpha(1-\theta)}\right),$$

$$\theta = \frac{(T-T_1)}{(T_2-T_1)}, \text{and } \Lambda = B_o \ exp\left(\frac{-\beta}{\alpha}\right).$$

The variable u is the velocity, p is the pressure, τ_{ij} is the stress tensor, q is the heat flux, e_t is the specific total internal energy, Y is the unburnt fuel mass fraction, $\dot{\omega}$ is the reaction rate, Q is the specific rate of reaction, T is the temperature, x_i refer to the spatial coordinates, t is the time, B_o is the pre-exponential factor, δ_{ij} is kronecker delta and Θ is the reduced temperature. The non-dimensional parameters used are Re=$(cL/v)_{ref}$, Pr=$(c_p\mu/\lambda)_{ref}$, Sc=$(vD)_{ref}$, Le=Sc/Pr, Da=$(D\Lambda/s_L^2)_{ref}$, $s_L^* = (s_L/c)_{ref}$ where v is the kinematic viscosity, c_p is the specific heat at constant pressure, λ is the thermal conductivity, μ is the dynamic viscosity, ρ is the density, D is the mass diffusion coefficient, Λ is the reduced pre-exponential factor, s_L is the laminar flame speed, Re is the acoustic Reynolds number, Pr is the Prandtl number, Sc is the Schmidt number, Le is the Lewis number, Da is the Damkohler number, δ_L is the flame thickness and s_L^* is the non-dimensional laminar flame speed. The subscript *ref* refers to unburnt gas properties which are treated as the reference condition. T_1 and T_2 refer to the temperatures of unburnt and burnt gases respectively. The heat release by the flame and the activation energy are measured by α and β respectively. The input parameters used in the simulation are Re=2000, Le=1, Pr=0.75, s_L/c_{ref}=0.016, T_b/T_u =4, α=0.75, β=8. The variables T_u and T_b refer to the unburnt and burnt gas temperatures respectively. These parameters are taken for a typical premixed flame simulated in Ref.[9].

Results and Discussions

Simple 1D transient simulation was performed initially, for the case of head-on quenching. The Peclet number (Pe) defined as the distance (y) of the flame from the wall, normalised by the reference flame thickness (δ_L), i.e. Pe=y/δ_L was calculated.

Quenching (minimum Pe in the domain) was found to occur at a Pe=3.6.

2D DNS was then conducted for the case of a steady flow. The contours of temperature and reaction rate for 2D steady flow are shown in Figure 2. The minimum Pe in this case was found to be 4.35 which is close to that in the 1D head-on quenching.

At high frequency of excitation (St=0.1), the flame does not respond strongly to the incoming velocity perturbations. The Pe number varies from 4.35 to 4.6, while the minimum Pe in the case of steady flame was found to be 4.35. This is expected as the flame position changes slightly in this case.

At an intermediate frequency of excitation (St=0.025), the flame is closest to the wall at t=0, with a Pe of 3.6 which is close to the value corresponding to head-on quenching (HOQ), reported earlier. At this instant, the flame has a long tail, parallel to the wall, making the flame-wall interaction more like a 1D head-on quenching. After extinction of this long tail, the flame starts to move backward with Pe number increasing until t=3(T/5). The flame then starts to move forward as the forcing of the inlet velocity goes into the positive side of the cycle. As illustrated in Figure 4, the flame continues to move away from the wall until the Pe number reaches its maximum value of 7. This value corresponds to the side-wall quenching (SWQ), as reported in the literature [9]. Afterwards, the flame developed a longer tail, while moving closer to the wall and the cycle starts again. The main observation from the flame behaviour at St=0.025 is that flame-wall interaction involves a combination of HOQ and SWQ.

In the case of low frequency of excitation (St=0.01), the flame moves away from the wall from t=0 to t=2(T/5) as Pe changes from 4.1 to 5.1, and moves towards the wall from t=3(T/5) onwards. At each value of Pe, the flame brushes along the X^+ direction, which is why there are multiple data points with the same Pe number (not all data points are shown for clarity). The minimum Pe in this case is 4.1, which is less than the value for steady flames (Pe=4.35). This indicates that the flame moves closer to the wall than a steady flame.
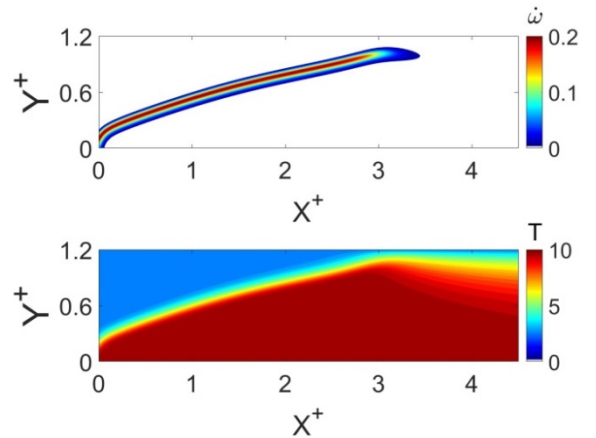
Figure 2: Contours of reaction rate and temperature (steady flame).
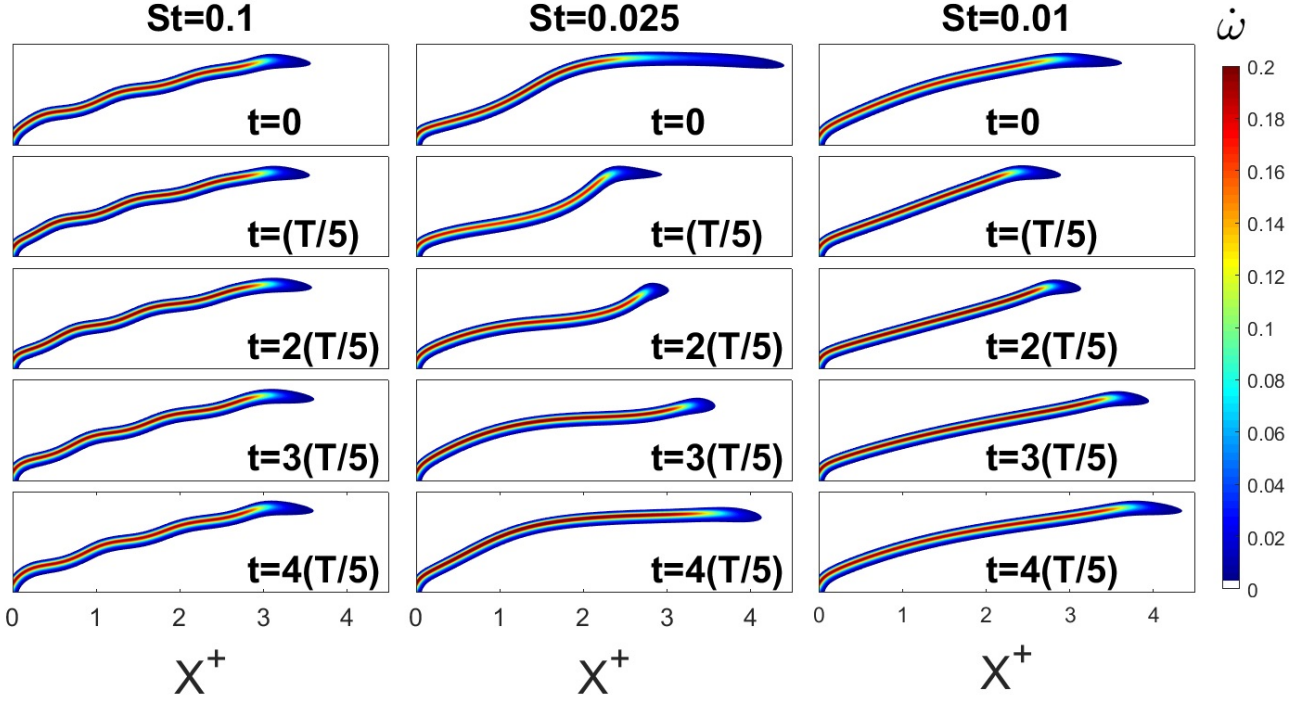
Figure 3: Snapshots of reaction rate contours at various times for St=0.01, 0.025 and 0.1 respectively.

The time-averaged mean and root mean square (RMS) values of wall heat flux (φ_{mean} and φ_{rms}), for different St, are plotted against X^+ in Figure 5. For clarity, only the plots of three selected frequencies are shown. Decreasing the excitation frequency spreads out the heat flux profile. In addition, higher RMS values are observed at lower excitation frequencies. This is expected since the flame travels a larger distance against the wall as the excitation frequency decreases. The RMS values of up to 50% of the mean values can be observed at low excitation frequencies showing a high level of heat flux fluctuations. The peak of the mean heat flux is located downstream of flame whereas the peak RMS is located closer to the inlet.

The variation of wall heat flux φ with time observed at the X^+ locations corresponding to maximum φ_{mean} and φ_{rms} were named $\varphi_{t,\ @max\ mean}$ and $\varphi_{t,\ @\ max\ rms}$, respectively. The mean with respect to time was deducted from $\varphi_{t,\ @max\ mean}$ and $\varphi_{t,\ @\ max\ rms}$, expressing the fluctuation of these two variables as $\varphi'_{t,\ @max\ mean}$ and $\varphi'_{t,\ @\ max\ rms}$. Also, the total wall heat flux φ_{total} for each time was calculated by integrating φ over X^+. The mean with respect to time was deducted from φ_{total}, and the fluctuation of total wall heat flux, was expressed as φ'_{total}. The Fourier transforms of $\varphi'_{t,\ @max\ mean}$, $\varphi'_{t,\ @\ max\ rms}$ and φ'_{total} were obtained to calculate the

amplitudes of these fluctuations, as shown in Figure 6.

The trend observed in this Figure 6 is consistent with what was reported earlier in the literature [8]. φ'_{total} shows a stronger variation with respect to the excitation frequency compared with $\varphi'_{t,\ @max\ mean}$ and $\varphi'_{t,\ @\ max\ rms}$. This suggests that the analysis of the wall heat flux at a single point may not be appropriate in the case of flame-wall interaction of forced flames.

Figure 6 shows that at high excitation frequencies, φ'_{total}, $\varphi'_{t,\ @max\ mean}$ and $\varphi'_{t,\ @\ max\ rms}$ converge to similar small values because the flame does not respond strongly to the incoming velocity perturbations. At an intermediate frequency, St =0.025, the maximum amplitude for the heat flux is observed. In particular, φ'_{total} is much higher than $\varphi'_{t,\ @max\ mean}$. At this frequency, $\varphi'_{t,\ @max\ mean}$ and $\varphi'_{t,\ @\ max\ rms}$ also show a peak. As discussed earlier, both HOQ and SWQ play a role during flame wall interaction for this case. At the lowest frequency of excitation, a comparable amplitude for φ'_{total} and $\varphi'_{t,\ @\ max\ rms}$ is observed. This is expected as the flame is mostly brushing against the wall at this frequency. Therefore, φ'_{total} will be mainly dominated by $\varphi'_{t,\ @\ max\ rms}$.
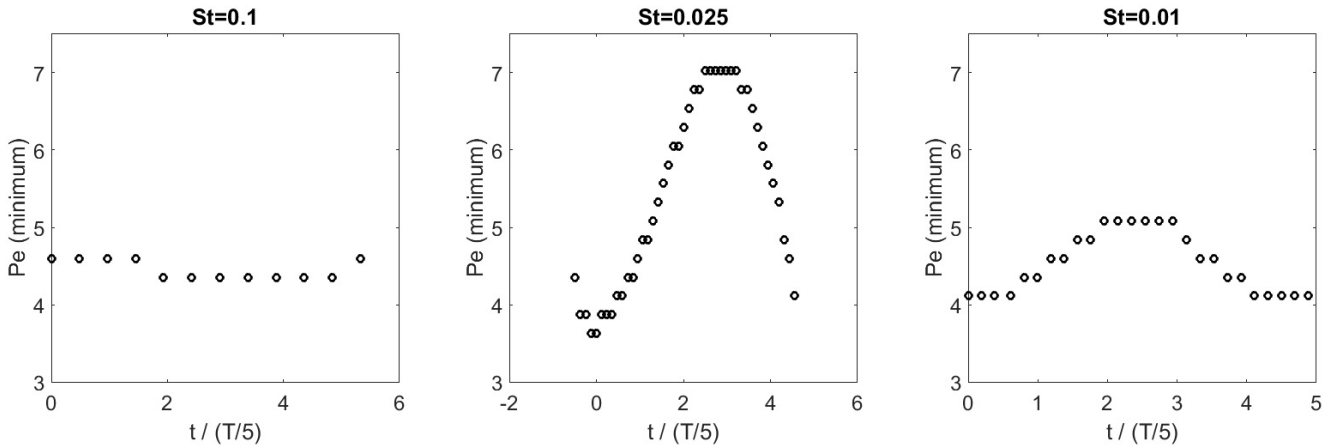
Figure 4: Minimum Pe number (minimum in the domain) vs time for St=0.01, 0.025 and 0.1 respectively.
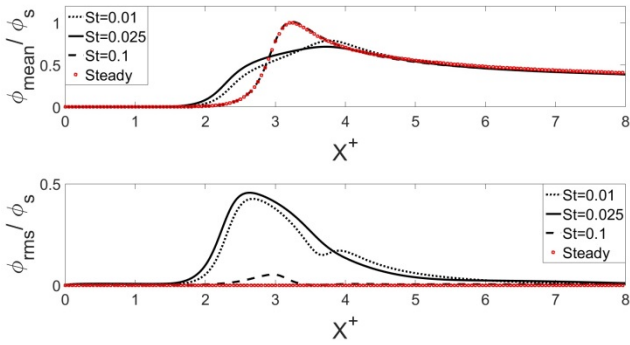
Figure 5: Mean and rms wall heat flux vs direction of flow (X^+) for different St (φ_s: maximum wall heat flux for steady flame).
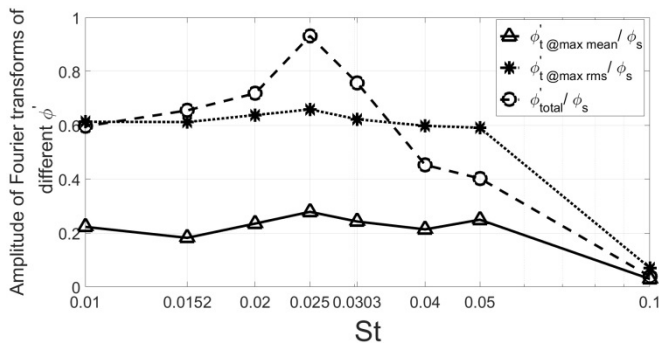
Figure 6: Amplitude of Fourier transforms of different φ', plotted in log-linear scale (φ_s: maximum wall heat flux for steady flame).

Conclusions

The present work investigated the flame behaviour near walls by studying the interaction of unsteady laminar premixed flames with a constant temperature wall. Two-dimensional DNSs of a forced flame were carried out for a range of excitation frequencies. To reduce the computational cost, a single-step chemistry model was used. The flame behavior was analysed in detail at St=0.01, 0.025 and 0.1. While the flame did not respond strongly at high frequency, it showed a brushing action at low frequency. The flame behaviour for intermediate frequencies showed a combination of head-on quenching and side-wall quenching. This behaviour resulted in significantly different trend of total wall heat flux from that of the wall heat flux calculated using conventional methods. This suggests that more consideration must be given to this calculation in order to appropriately characterise the flame behaviour.

Acknowledgments

References

1. Bellenoue, M., T. Kageyama, S. Labuda, & J. Sotton, Direct measurement of laminar flame quenching distance in a closed vessel. *Experimental Thermal and Fluid Science*, 2003. **27**(3): p. 323-331.

2. Bourlioux, A., B. Cuenot, & T. Poinsot, Asymptotic and numerical study of the stabilization of diffusion flames by hot gas. *Combustion and Flame*, 2000. **120**(1): p. 143-159.

3. Bruneaux, G., K. Akselvoll, T. Poinsot, & J. Ferziger, Flame-wall interaction simulation in a turbulent channel flow. *Combustion and Flame*, 1996. **107**(1): p. 27-44.

4. Cuenot, B., B. Bedet, & A. Corjon, NTMIX3D user's guide manual. *Preliminary Version 1*, 1997.

5. Dabireau, F., B. Cuenot, O. Vermorel, & T. Poinsot, Interaction of flames of $H_2 + O_2$ with inert walls. *Combustion and Flame*, 2003. **135**(1): p. 123-133.

6. Dreizler, A. &B. Böhm, Advanced laser diagnostics for an improved understanding of premixed flame-wall interactions. *Proceedings of the Combustion Institute*, 2015. **35**(1): p. 37-64.

7. Enomoto, M., Sidewall quenching of laminar premixed flames propagating along the single wall surface. *Proceedings of the Combustion Institute*, 2002. **29**(1): p. 781-787.

8. Gruber, A., R. Sankaran, E. Hawkes, & J. Chen, Turbulent flame–wall interaction: a direct numerical simulation study. *Journal of Fluid Mechanics*, 2010. **658**: p. 5-32.

9. Poinsot, T., D. Haworth, & G. Bruneaux, Direct simulation and modeling of flame-wall interaction for premixed turbulent combustion. *Combustion and Flame*, 1993. **95**(1): p. 118-132.

10. Poinsot, T.J. &S. Lele, Boundary conditions for direct simulations of compressible viscous flows. *Journal of Computational Physics*, 1992. **101**(1): p. 104-129.

11. Popp, P. &M. Baum, Analysis of wall heat fluxes, reaction mechanisms, and unburnt hydrocarbons during the head-on quenching of a laminar methane flame. *Combustion and Flame*, 1997. **108**(3): p. 327-348.

12. Talei, M., M.J. Brear, & E.R. Hawkes, A parametric study of sound generation by premixed laminar flame annihilation. *Combustion and Flame*, 2012. **159**(2): p. 757-769.

13. Talei, M., M.J. Brear, & E.R. Hawkes, Sound generation by laminar premixed flame annihilation. *Journal of Fluid Mechanics*, 2011. **679**: p. 194-218.